The VanS sensor histidine kinase from type-B VRE recognizes vancomycin directly

Lina J. Maciunas,[a,1] Photis Rotsides,[a,1] Samantha Brady,[a] Joris Beld,[b] Patrick J. Loll[a,*]

Departments of Biochemistry & Molecular Biology[a] and Microbiology and Immunology[b], Drexel University College of Medicine, Philadelphia, PA 19102 USA

[1] LJM and PR contributed equally to this work

* To whom correspondence may be addressed:

Patrick J. Loll
Department of Biochemistry and Molecular Biology
Drexel University College of Medicine
245 N. 15th St., MS 497
Philadelphia, PA 19102 USA
Email: pjl28@drexel.edu

Author Contributions: LJM, PR, and PJL designed research; LJM, PR, SB, JB, and PJL performed research; LJM, PR, JB, and PJL analyzed data; and LJM, PR, and PJL wrote the paper.

Competing Interest Statement: Nothing to disclose.

Keywords: Vancomycin; antibiotic resistance; vancomycin-resistant Enterococci; two-component system

Abstract

Vancomycin-resistant enterococci (VRE) are among the most common causes of nosocomial infections, which can be challenging to treat. VRE have acquired a suite of resistance genes that function together to confer resistance to vancomycin. Expression of the resistance phenotype is controlled by the VanRS two-component system. This system senses the presence of the antibiotic, and responds by initiating transcription of resistance genes. VanS is a transmembrane sensor histidine kinase, and plays a fundamental role in antibiotic resistance by detecting vancomycin and then transducing this signal to VanR. Despite the critical role played by VanS, fundamental questions remain about its function, and in particular about how it senses vancomycin. Here, we focus on purified VanRS systems from the two most clinically prevalent forms of VRE, types A and B. We show that in a native-like membrane environment, the enzymatic activities of type-A VanS are insensitive to vancomycin, suggesting that the protein functions by an indirect mechanism that detects a downstream consequence of antibiotic activity. In contrast, the autokinase activity of type-B VanS is strongly stimulated by vancomycin. We additionally demonstrate that this effect is mediated by a direct physical interaction between the antibiotic and the type-B VanS protein, and localize the interacting region to the protein's periplasmic domain. This represents the first time that a direct sensing mechanism has been confirmed for any VanS protein.

Significance Statement

When vancomycin-resistant enterococci (VRE) sense the presence of vancomycin, they remodel their cell walls to block antibiotic binding. This resistance phenotype is controlled by the VanS protein, a sensor histidine kinase that senses the antibiotic and signals for transcription of resistance genes. However, the mechanism by which VanS detects the antibiotic has remained unclear. Here, we show that VanS proteins from the two most common types of VRE use very different sensing mechanisms. Vancomycin does not alter the signaling activity of VanS from type-A VRE, suggesting an indirect sensing mechanism; in contrast, VanS from type-B VRE is activated by direct binding of the antibiotic. Such mechanistic insights will likely prove useful in circumventing vancomycin resistance.

INTRODUCTION

Antibiotic resistance is a global health problem. Pathogenic bacteria are becoming resistant to currently available antibiotics at an alarming rate, while the development of new antibiotics is slow (1). Important examples of antibiotic-resistant bacteria include the vancomycin-resistant enterococci (VRE), which have been identified by the World Health Organization as top priorities for new therapeutic development (2, 3). VRE are among the so-called ESKAPE pathogens; these organisms are leading causes of hospital-acquired infections, and few therapeutic options remain for their treatment (4, 5).

VRE evade vancomycin's antibiotic action by remodeling their cell wall, preventing the antibiotic from binding its target (6). This mode of resistance requires the acquisition of five key genes, *vanRSHAX,* which are necessary and sufficient to confer vancomycin resistance (7). VanHAX are enzymes that remodel vancomycin's cell-wall target, and their expression is controlled by a two-component system comprising VanR and VanS. VanR is a transcription factor that is activated by phosphorylation; VanS is a membrane-bound sensor histidine kinase that detects vancomycin and modulates the phosphorylation state of VanR accordingly (8).

VanS proteins, like many other sensor histidine kinases, consist of four structural domains: a sensor domain, a membrane-proximal domain, a dimerization-and-histidine phosphotransfer (DHp) domain, and a catalytic and ATP-binding (CA) domain (9, 10) (Figure 1A). The sensor domain contains two transmembrane helices flanking a periplasmic region (11, 12), and is responsible for recognizing the presence of vancomycin. When VanS senses vancomycin, the signal is transduced to the cytoplasmic domains, which coordinate an enzymatic response involving autophosphorylation on a conserved histidine residue, followed by transfer of the phosphoryl group to VanR. Once phosphorylated, VanR initiates transcription of the resistance genes. In the absence of an activating signal, VanS can dephosphorylate VanR, terminating the signaling cascade. Interrupting this signaling process, either by inhibiting autophosphorylation and phosphotransfer, or by stimulating VanR dephosphorylation, represents an obvious therapeutic avenue that could salvage the utility of the antibiotic.

The largest gap in our understanding of vancomycin resistance centers on how VanS recognizes vancomycin. In principle, VanS could detect vancomycin either directly, via a physical interaction with the antibiotic, or indirectly, by sensing a downstream consequence of vancomycin action. Arguments have been advanced in favor of both possibilities. Chimeric-protein studies, photolabeling, and spectroscopic experiments have all provided data that support a direct-interaction model (13-18); in contrast, an indirect model is supported by the observation that VanS can be promiscuously activated by many different inhibitors of cell-wall biosynthesis (based on the reasoning that a single binding site on VanS would be unlikely to recognize a wide array of structurally dissimilar effectors) (19-22). Importantly, the direct and indirect models are not necessarily mutually exclusive, nor must a single model apply to all VanS proteins. Thus, considerable uncertainty surrounds the molecular mechanism by which VanS recognizes and transduces the vancomycin signal.

To elucidate this process, we have purified full-length VanS proteins and inserted them into nanodiscs, thereby providing the molecular insights that can be achieved by reconstituting a signaling system from purified components, while simultaneously maintaining a native-like membrane environment. Focusing on VanS proteins from the two most clinically relevant VRE types, A and B (denoted herein as $VanS_A$ and $VanS_B$), we investigated the relationship of

vancomycin binding to enzymatic activity. We demonstrate that $VanS_A$ and $VanS_B$ respond differently to vancomycin, with the antibiotic having no effect on $VanS_A$ activity, but markedly stimulating $VanS_B$ activity. We further demonstrate a direct physical interaction between the $VanS_B$ sensor domain and vancomycin, linking activity changes with direct binding of the antibiotic for the first time for any VanS protein.

RESULTS

Reconstitution of VanS into nanodiscs

Membrane proteins are typically purified in detergent-solubilized form, but detergents can reduce stability and/or block access to interaction sites (23-25). The latter effect is of particular concern in the VanRS system, since it has been suggested that vancomycin interacts with VanS at a site directly adjacent to the membrane (16). To provide a more native-like environment for VanS proteins, we reconstituted them into nanodiscs, lipid-bilayer discs belted by an amphipathic scaffolding protein (26, 27). VanS nanodiscs were created by mixing detergent-solubilized VanS with *E. coli* lipids and the scaffolding protein MSP1D1, after which detergent was removed, allowing the nanodiscs to spontaneously assemble (Figure 1B). VanS-containing nanodiscs were separated from empty nanodiscs by capturing the His-tagged VanS protein via nickel-affinity chromatography, after which aggregated material was removed on a size-exclusion column. Re-injection of the purified material gave symmetrical peaks eluting significantly earlier than empty nanodiscs (Figure 1C). SDS-PAGE analysis revealed that VanS and MSP1D1 are present in the nanodiscs in an approximate 1:1 stoichiometry (Figure 1D). Since each disc is known to contain two copies of the MSP1D1 scaffolding protein (27), this implies that on average, each nanodisc contains a single VanS homodimer. These reconstituted VanS proteins provide the foundation for the following *in vitro* experiments, allowing us to avoid the complications associated with the use of detergent.

VanS proteins are active after reconstitution into nanodiscs

Sensor histidine kinases autophosphorylate in response to signals; they also modulate the phosphorylation states of their response regulators, transferring their phosphoryl group to the response regulator. Some sensor kinases exert additional control via a phosphatase activity that dephosphorylates their response regulators in the absence of a signal (28). These three activities reside in the cytosolic domains of the kinases, and are regulated by the transmembrane and sensor regions in response to stimulus detection. Constructs containing only the cytosolic domains of $VanS_A$ and $VanS_B$ display all three enzymatic activities, as does detergent-solubilized full-length $VanS_A$ (29-31). To examine VanS activity in a nanodisc environment, we first focused on the autophosphorylation function. We monitored activity using a modified Western blot assay (Figure 2A), in which VanS was allowed to autophosphorylate with ATPγS, after which the thiophosphohistidine was alkylated and detected by antibody (32). Both $VanS_A$ and $VanS_B$ are strongly sensitive to the specific membrane-mimetic used, with both showing essentially no activity in the presence of the detergents dodecyl maltoside (DDM) or lauryl dimethyl amine oxide (LDAO), and modest activity in dodecyloctapolyoxyethylene ($C_{12}E_8$). In contrast, the nanodisc preparations of $VanS_A$ and $VanS_B$ are both autokinase-active, validating our use of this approach. However, the behaviors of the two proteins differ in their details. Once reconstituted into nanodiscs, $VanS_A$

showed a dramatic increase in autophosphorylation activity, whereas $VanS_B$ showed only a small activity increase.

We next probed dephosphorylation activity, incubating $VanS_A$ and $VanS_B$ with the phosphorylated forms of their cognate VanR proteins, and quantifying the time-dependent decrease in phospho-VanR using Phos-tag™ gels (33, 34). Both proteins showed dephosphorylation activity versus their respective response regulators, with the $VanS_B$ protein catalyzing slightly more rapid dephosphorylation than $VanS_A$ (Figure 2B, 2C).

We did not quantify phosphotransfer activity, since the catalytic machinery mediating this process typically resides primarily in the response regulator, rather than the sensor kinase (35). We have confirmed, however, that $VanS_A$ and $VanS_B$ are both capable of phosphotransfer to their cognate VanR partners ((31); SI Appendix, Fig. S1).

Hence, our reconstituted nanodisc preparations possess the relevant enzymatic activities. However, the activities of the proteins differ subtly, with $VanS_A$'s autophosphorylation activity being dramatically higher in the nanodiscs than in detergents, while $VanS_B$ showed equivalent activities in both environments. In the nanodisc environment, the overall level of $VanS_A$ autokinase activity is much higher than that of $VanS_B$, while $VanS_A$ showed substantially lower phosphatase activity than $VanS_B$. Taken together, these differences in activities suggest that nanodisc $VanS_A$ has been captured in a more activated state than $VanS_B$.

Vancomycin's effect on VanS activity

We hypothesized that if vancomycin directly activates VanS, then the antibiotic should either increase the enzyme's autokinase activity and/or decrease its phosphatase activity; either effect would tend to increase cellular levels of phospho-VanR. We first investigated the effect of vancomycin on the autophosphorylation activities of $VanS_A$ and $VanS_B$. We found that while vancomycin had no effect on the autophosphorylation activity of $VanS_A$, it stimulated $VanS_B$ autophosphorylation in a concentration-dependent manner (Figure 3A & 3B). We then showed that this stimulatory effect was also observed using ^{32}P-ATP as a kinase substrate, confirming that this result was not unique to ATPγS (SI Appendix, Fig. S2).

When VanS is embedded in a nanodisc, both its extracellular and intracellular domains will be accessible to a water-soluble molecule such as vancomycin; however, in the native cellular environment, only the periplasmic domain will be accessible to the antibiotic. Therefore, any effect that vancomycin has on the enzyme's activity should be mediated through the periplasmic sensor domain, and not through any of the cytosolic domains. To confirm the absence of any such nonspecific effects, we purified a $VanS_B$ construct lacking the sensor domain, and showed that vancomycin has no effect on its autophosphorylation activity (Figure 3C, SI Appendix Fig. S3). Thus, the stimulatory effect of vancomycin is specific to the full-length $VanS_B$ protein.

Finally, we tested whether vancomycin influences the dephosphorylation activities of the VanS proteins, and found minimal effects. Specifically, vancomycin had no effect on the dephosphorylation activity of $VanS_A$, while it slightly decreased the dephosphorylation activity of $VanS_B$ (Figure 3D-G). In summary, vancomycin increases $VanS_B$'s autophosphorylation activity and modestly decreases its phosphatase activity; both effects are consistent with vancomycin directly stimulating VanRS signaling in type-B VRE. In contrast, vancomycin has no appreciable effect on the enzymatic activities of $VanS_A$.

Vancomycin binds to the periplasmic sensor domain of $VanS_B$

Vancomycin's effect on the enzymatic activity of purified $VanS_B$ suggests that the antibiotic might bind directly to the enzyme. We reasoned that the likely site of binding is the protein's periplasmic region, as it is the only portion of the protein accessible from the outside of the cell. The $VanS_B$ periplasmic domain contains roughly 100 residues, and it is predicted to adopt a PAS-domain fold (SI Appendix, Fig. S4) (36, 37). To test whether the isolated periplasmic domain is capable of binding the antibiotic, we prepared expression constructs for the appropriate region, corresponding to $VanS_B$ residues 31-132. We produced two constructs, the first encoding a single copy of the periplasmic sensor, and the second containing two copies of the sensor in tandem, separated by a short linker (Figure 4A). The latter construct was designed to encourage dimerization, since full-length sensor histidine kinases are thought to be obligate dimers (28). Both proteins were purified to homogeneity (SI Appendix, Fig. S4A).

We first probed antibiotic binding to the periplasmic-domain constructs using two novel photoaffinity probes, one in which the diazirine photolabel is attached to the antibiotic's vancosamine sugar (Probe V), and one in which it is attached to the antibiotic's N-terminus (Probe N; see Figure 4B) (38). Both photoprobes efficiently labeled the tandem $VanS_B$ sensor protein, as demonstrated by mass spectrometry and anti-vancomycin Western blotting (Figure 4C-E). No evidence was seen for double labeling of the tandem sensor domain, even though in principle it can contain two distinct ligand-binding sites (39); however, a dimer is not required for the interaction, since photolabeling was also observed for the single-copy sensor. Unlabeled vancomycin competed effectively with both photoprobes, demonstrating specificity for the protein-photoprobe interaction. Notably, both photoprobes also label the full-length $VanS_B$ protein, indicating that the observed interaction with the sensor domain is not an artifact caused by removing the periplasmic domain from the context of the intact protein molecule. Overall, these results provided strong evidence of a specific, direct interaction between vancomycin and the $VanS_B$ protein.

We next sought to quantify this binding interaction, using fluorescence anisotropy to assess recognition of BODIPY-labeled vancomycin (Figure 5). The single-copy $VanS_B$ sensor domain was found to bind to the labeled vancomycin with a dissociation constant (K_D) of 20.3 μM, while the tandem sensor bound with a K_D of 10.7 μM; the fact that the single-domain K_D value is almost exactly twice that of the tandem domain suggests that there is no cooperativity between the two domains, at least in the constructs used. We then generated negative controls, creating single- and tandem-domain versions of the periplasmic sensor domain from the *B. subtilis* histidine kinase PhoR. The PhoR sensor domain adopts a PAS fold, similar to that predicted for the $VanS_B$ periplasmic domain (40), but PhoR should not bind to vancomycin, and, as expected, neither PhoR construct bound to BODIPY-vancomycin (Figure 5B). Next, to test whether the binding observed in the anisotropy experiment was fluorophore-dependent, we created a new fluorescent probe by labeling vancomycin with AlexaFluor488 at the vancosamine sugar (Figure 5A,C). The tandem $VanS_B$ sensor protein bound to AF488-vancomycin with a K_D value of 11.0 μM, in good agreement with the affinity for BODIPY-vancomycin. Both of these probes have the fluorophore attached at the same position, but AlexaFluor-488 differs significantly from BODIPY in both structure and hydrophobicity; hence, these results demonstrate that the observed binding cannot be ascribed to nonspecific interactions with the fluorophore. Finally, we used isothermal titration calorimetry (ITC) to measure the binding of label-free vancomycin to the $VanS_B$ sensor domain, obtaining a K_D of

20.7 μM for the single-copy sensor domain, in excellent agreement with the results of the fluorescence-anisotropy experiments (Figure 5D). Importantly, the related glycopeptide antibiotic teicoplanin does not bind the $VanS_B$ sensor (SI Appendix, Fig. S5), consistent with observation that teicoplanin does not induce resistance in type-B VRE (20). Taken together, these results clearly demonstrate a direct and specific binding interaction between vancomycin and the periplasmic sensor domain of $VanS_B$.

Discussion

The mechanism by which VRE evade vancomycin remains incompletely understood, with the largest open questions being how VanS recognizes the antibiotic and transduces this signal. Answers to these questions will likely inform the development of new therapeutic avenues. Here, we have begun to address these issues, studying the VanS proteins from the two most clinically relevant VRE types.

Previous studies of the effect of vancomycin upon the activity of $VanS_A$ have yielded varying results; one exhaustive study of all three activities in both detergents and amphipols saw no appreciable effect of vancomycin on any enzymatic activity (31), while another study suggested that the antibiotic modestly enhanced the rate of ATP hydrolysis (13). In case these inconsistencies resulted from differences in the membrane-mimetic environment, we chose to reconstitute $VanS_A$ into nanodiscs, in order to provide the enzyme with a native-like lipid environment. Only a small number of sensor histidine kinases have been reconstituted into nanodiscs (41-48), and this is the first report of this approach being applied to any VanS protein. Interestingly, even in a native-like membrane environment, $VanS_A$ activity is insensitive to vancomycin, which is an argument in favor of an indirect-activation model for this protein, implying that the activating signal is not vancomycin *per se*, but rather some downstream consequence of vancomycin activity. The precise nature of such a signal remains unclear, but could be related to our observation that $VanS_A$'s activity state is extremely sensitive to the lipid environment; this might suggest that $VanS_A$ activity is modulated by cell-envelope stress or changes in membrane fluidity (39, 49). Alternatively, vancomycin's failure to alter the activity of purified $VanS_A$ may indicate that some unknown regulatory component is missing from the reconstituted system. For example, the high levels of autokinase activity observed for $VanS_A$ might hint that our preparations lack an inhibitor, such an associated membrane-bound partner (50) or a transmembrane regulatory peptide (51-53).

In contrast to $VanS_A$, the full-length $VanS_B$ protein had not been well characterized prior to this work, and here we demonstrate that it responds to vancomycin very differently than does $VanS_A$. Specifically, while vancomycin has no effect on $VanS_A$, it increases $VanS_B$'s autophosphorylation activity and slightly decreases its phosphatase activity; both effects will lead to increased levels of phospho-$VanR_B$, thereby stimulating the transcription of the resistance operon. We further provide evidence of a direct physical interaction between vancomycin and $VanS_B$. This is the first time that direct binding of the antibiotic has been linked to activity changes in a VanS protein.

While we observe clear evidence for vancomycin binding to the $VanS_B$ sensor domain, the affinities and EC50 value are significantly higher than the ~2 μM vancomycin concentration required to induce transcription of resistance genes in VRE-B (20). This disparity suggests that our *in-vitro* system, while useful, is not a perfect mimic of the environment found *in vivo*. For example, our

nanodiscs contain one $VanS_B$ dimer per disc; if a higher-order assembly of dimers is required for complete activation (41), this could not be achieved in our system. Another factor to consider is the lipid composition of our nanodiscs. Our preparations used commercially available *E. coli* lipids, in which phosphatidylethanolamine is the predominant lipid species, along with smaller amounts of phosphatidylglycerol and cardiolipin (54). In contrast, membranes of Enterococci feature primarily phosphatidylglycerol and cardiolipin (55). Additionally, lipid II accumulates in response to vancomycin's antibiotic activity (56), but is absent from our nanodisc preparations; a build-up of lipid II could modulate the effects of vancomycin on $VanS_B$ activity, perhaps by recruiting the antibiotic to the vicinity of the membrane-proximal sensor domain.

$VanS_A$ and $VanS_B$ perform equivalent functions in their respective VRE strains, but function by different mechanisms. The key to these mechanistic differences appears to reside in the two proteins' sensor domains. $VanS_A$ and $VanS_B$ share ~19% sequence identity and 36% similarity overall, but the similarities are most pronounced in the cytoplasmic domains, while the periplasmic domains are highly dissimilar in both size and sequence. For example, the $VanS_A$ periplasmic domain contains only ~37 residues, as compared to ~101 residues in the corresponding $VanS_B$ domain (SI Appendix, Fig. S6). Phylogenetic analysis reveals that VanS genes from type-B VRE form an outlier cluster, distinct from the VanS genes associated with other VRE types (57); indeed, the VanS sequences from all non-B VRE types are more similar to one another than any of them are to type-B sequences. The presence of a periplasmic PAS domain appears to be unique to type-B VanS proteins, with VanS proteins from all other VRE types having considerably shorter sequences in their periplasmic regions (SI Appendix, Fig. S7). Hence, it appears the type-B vancomycin-resistance operon contains an evolutionarily distinct feature that allows VanS to bind directly to vancomycin, and this feature is not shared by VanS proteins from other VRE types.

Materials and Methods

Expression constructs. Primers used for subcloning can be found in Table S1. pMSP1D1 was obtained from Addgene (catalog #20061). The genes for full-length $VanS_B$ and $VanR_B$ were codon-optimized for expression in *E. coli* cells by Genscript (Piscataway, NJ) and subcloned into the in-house pETCH vector, producing expression constructs containing C-terminal His_6 tags (58). The cytosolic form of $VanS_B$ ($cVanS_B$) was previously determined to comprise residues M159-L447 (30), and the corresponding gene fragment was subcloned into pETCH. The periplasmic domain of $VanS_B$ is located between the two transmembrane helices, which are predicted to consist of residues 10-28 and 135-155 (59). Therefore, to produce a tandem periplasmic-domain construct, two gene fragments were designed. Both encoded residues Q31 to G132 of VanSB, and also included an overlapping linker region encoding the linker sequence GSGGS connecting the C-terminus of the first copy to the N-terminus of the second copy. These fragments were assembled using the NEBuilder HiFi Assembly kit into pMal-c6T (NEB #N0378S). The resulting construct encodes a TEV-cleavable 6xHis-MBP tag fused to two copies of the $VanS_B$ periplasmic domain. The single-copy construct was created by introducing the sequence TAAT via a site-directed mutagenesis, placing an enhanced stop codon after the first copy of the $VanS_B$ sensor domain (60). A similar strategy was used to produce tandem and single-copy constructs of the *B. subtilis* PhoR periplasmic domain (Uniprot P23545 aa 32-150), amplifying the appropriate region from *Bacillus subtilis* subsp. *subtilis* strain 168 (ATCC cat. no. 23857).

Protein expression and purification. $VanS_A$ and $VanS_B$ were purified as previously described (31) with minor modifications. Briefly, pelleted cells from 6-L cultures were resuspended in IMAC-A buffer (40 mM Tris pH 8, 300 mM NaCl, 25 mM imidazole) containing EDTA-free protease inhibitor tablets (Thermo-Pierce) and then lysed in a C5 Emulsiflex cell homogenizer at 10,000-15,000 psi. Membranes were isolated by centrifugation and homogenized in IMAC-A buffer, after which proteins were solubilized by the addition of 1% (w/v) *N*-dodecyl-β-D-maltopyranoside (DDM) for 1 hour at 4°C. The solubilized membranes were centrifuged at 150K *g* for 50 min, and the resulting supernatant was syringe-filtered (0.45 µm) and loaded onto a 1-mL IMAC-HP column (Cytiva) equilibrated in IMAC-A buffer containing 0.2% DDM. Protein was eluted with a gradient from 25 to 350 mM imidazole.

$VanR_B$ was co-expressed with GroEL/S chaperones. pETCH-$VanR_B$ and pGro7 (Takara Cat# 3340) were cotransformed into BL21(DE3) cells. Overnight cultures were diluted 1:500 in LB media containing 100 µg/mL ampicillin and 34 µg/mL chloramphenicol. Immediately after inoculation, arabinose (1 mg/mL) was added to induce chaperone expression. At OD600 = 0.5, the temperature was lowered to 30°C, IPTG was added (0.2 mM), and cells were incubated for 4 hours. Cells harvested from 3-L cultures were resuspended in 40 mM Tris pH 8, 500 mM NaCl, 25 mM imidazole, 10% w/v glycerol, 5 mM $MgCl_2$ (Buffer IMAC-A2) containing 10 µg/mL DNase, 2 µg/mL RNase, and EDTA-free protease inhibitor tablets. The resuspended cells were lysed by homogenization, after which Triton-X100 was added to the lysate at a final concentration of 0.1% (v/v) and the sample incubated at 4 °C for 1 hour. The lysate was centrifuged at 150K *g* for 1 hour, filtered (0.45-µm), and loaded onto a 1-mL IMAC-HP column equilibrated in IMAC-A2 containing 0.1% Triton-X100. The column was washed with 20 CV of IMAC-A2 containing 0.1% Triton-X100, 20 CV of IMAC-A2 without detergent, and 20 CV of 10% IMAC-B2 (40 mM Tris pH 8, 500 mM NaCl, 350 mM imidazole, 10% glycerol, 5 mM $MgCl_2$). $VanR_B$ was eluted with a gradient from 10-100% IMAC-B2. Fractions containing $VanR_B$ were pooled, concentrated to 5 mL, syringe-filtered (0.22-µm), and injected onto a Sephacryl S300 16/60 size-exclusion column (Cytiva) equilibrated in

IMAC-A2 buffer lacking imidazole. Aliquots of $VanR_B$ were flash-frozen in liquid nitrogen and stored at -80°C.

All periplasmic-domain constructs were expressed in BL21(DE3) cells. Cells were grown in LB broth with 0.2% glucose at 37°C to an OD_{600} of ~0.6, at which point temperature was reduced to 16°C and IPTG was added to a final concentration of 200 μM. Cells were harvested after ~22 hours of shaking at 225 RPM. Cells from two-liter growths were lysed in buffer containing 20 mM Tris pH 7.5, 200 mM NaCl, 5 mM $MgCl_2$, 1mM EDTA, and protease inhibitors (ThermoFisher #A32963). Cell lysate was clarified by centrifugation at 10,000x*g* for 20 minutes then at 117,000x*g* for one hour, after which the soluble supernatant was filtered (0.45 μm) and loaded onto a 42-mL column packed with amylose resin (NEB #E8021L) equilibrated with Buffer A3 (20mM Tris pH 7.5, 100mM NaCl). The column was washed with Buffer A3, then the captured protein was eluted in batch using Buffer A3 supplemented with 50 mM maltose. The eluted protein was mixed with 2 mg of TEV protease and dialyzed overnight against one liter of IEX buffer (20 mM Tris pH 7.5) with 1mM DTT. The following day, the dialysate was loaded onto a 5-mL HiTrap Q HP column (Cytiva) equilibrated with IEX buffer. The column was first washed with IEX buffer, followed by IEX buffer supplemented with 100 mM NaCl. At this point, a 5-mL HiTrap IMAC HP column was attached downstream of the Q column and proteins were eluted using IEX buffer containing 600 mM NaCl. The IMAC column served to capture the TEV protease, the cleaved 6xHis-MBP tag, and any uncleaved protein during elution. The eluted protein was concentrated to 10 mL and loaded onto a Sephacryl-S100 26/60 column equilibrated with Buffer A3. Fractions containing the desired proteins were analyzed by SDS-PAGE for purity, pooled, and concentrated to at least 5 mg/mL.

$cVanS_B$ was purified similarly to $VanR_B$ with one modification: 21 mM *N*-decyl-*N*,*N*-dimethylamine-*N*-oxide (DDAO) was added to the lysate and buffer IMAC-A2. MSP1D1 was expressed and purified as previously described (26, 27).

Nanodisc Assembly and Purification

4 mL of a chloroform solution of *E. coli* total lipid extract (Avanti Polar Lipids, Inc.) were placed in a clean glass vial. The chloroform was evaporated with a stream of N_2 gas and the vial placed in a lyophilizer overnight. The dried lipids were resuspended in 3.75 mL of 4% (w/v) DDM in ultrapure water. The suspension was sonicated for 10 min, freeze-thawed, sonicated for an additional 10 min, and then stored on ice. Lipid concentration was determined by phosphorous assay (61, 62). Nanodiscs were assembled by combining VanS, MSP1D1, and *E. coli* lipids in a mole ratio of 1:10:600 in a final volume of 500 μl, with a final VanS concentration of 4 μM. After a 40-min incubation at room temperature, the 500-μl nanodisc mixture was added to 200 μl wet Bio-BeadsTM (Bio-Rad Cat# 1523920) in a fresh 1.5-mL tube. Bio-BeadsTM were prepared as described in (63). The BioBead-containing mixtures were rotated end-over-end at 4°C overnight. The following day, Bio-Beads were removed by filtration and the concentration of imidazole was reduced to 30 mM by diluting the sample with cold ND buffer (20 mM Tris pH 7.4,150 mM NaCl). The sample was syringe-filtered (0.22 μm) and applied to a gravity-flow column containing a 600-μl bed volume of charged nickel resin equilibrated in IMAC A buffer. The column was washed with 4 mL of cold IMAC A and the VanS-containing nanodiscs were eluted with 1.8 mL of cold 50% IMAC B buffer. The eluate was concentrated to 250 μl using a 100-kDa MWCO 0.5-mL concentrator, filtered (0.22 μm), and injected onto a Superdex 200 10/300 column (Cytiva)

equilibrated in ND buffer at room temperature. Peak fractions were pooled, concentrated, quantified, and used for activity assays.

Autophosphorylation Assays. The autophosphorylation assays using ATPγS were performed as described (31). Briefly, VanS was incubated in 50 mM KCl, 10 mM $MgCl_2$, 50 mM Tris pH=7.4 with 1 mM ATPγS for specified times, after which the reaction was quenched by addition of EDTA and PNBM was added to alkylate the thiophosphohistidine. Samples were analyzed by SDS-PAGE and Western blotting, probing with an anti-PNBM antibody (Abcam ab92570). Detailed methods are provided in the Supporting Information.

Autophosphorylation experiments using γ–^{32}P-labeled ATP (PerkinElmer BLU002Z250UC, 10mCi/mL) were set up similarly to those using ATPγS. A 50-µL autophosphorylation reaction contained 1X reaction buffer, 2 µL of the ^{32}P-ATP stock, 1 mM cold ATP, and $VanS_B$-containing nanodiscs at 0.5 µM. Reactions were quenched by the simultaneous addition of EDTA and SDS-PAGE loading buffer and the samples analyzed by SDS-PAGE.

Dephosphorylation Assays. Dephosphorylation was assessed by incubating partially phosphorylated VanR protein with the cognate VanS; the reaction was quenched at various time points by the addition of SDS-PAGE loading buffer, after which samples were analyzed by electrophoresis on Phos-tag™ gels (Fujifilm Cat. # 195-17991). Additional details are provided in the Supporting Information.

Photolabeling Reactions. Photoprobes containing diazirine groups attached to either the amino group of vancomycin's vancosamine sugar (Probe V) or to the antibiotic's N-terminus (Probe N) were prepared as described (38). Photolabeling was initiated by irradiation with 365-nm light, and samples were analyzed by mass spectrometry and Western blotting; details are provided in the Supporting Information.

Vancomycin Binding Assays. Fluorescence anisotropy experiments were conducted in 20-µL volumes containing 100 nM BODIPY-vancomycin (ThermoFisher #V34850) or Alexa Fluor 488-vancomycin in 20 mM Tris pH 7.5 buffer containing 100 mM NaCl and 0.01% Triton X-100, using black 384-well small-volume plates (Greiner Bio-One # 784077). Anisotropy measurements were conducted at room temperature using a Tecan Spark microplate reader. Samples were excited at 490 nm and emission read at 525 nm, using a 10 nm bandpass for both emission and excitation. A 510 nm dichroic mirror was used to condition the emitted signal.

ITC experiments were carried out using a MicroCal VP-ITC calorimeter (Malvern Panalytical). Protein and vancomycin stock solutions were exhaustively dialyzed against 20 mM Bicine pH 7.5. The sample cell was filled with 200 µM vancomycin and the injection syringe was loaded with 2 mM $VanS_B$ single-copy periplasmic-domain protein. An initial 5-µL injection was followed by twenty 10-µL injections at 15°C, with four minutes between each injection and spinning at 340 RPM. Binding signatures were analyzed using the MicroCal Analysis software and the data were fit using a single-site model.

Acknowledgements

This work was supported in part by grant 1R01AI148679 from the National Institute of Allergy and Infectious Disease, National Institutes of Health. The authors gratefully acknowledge Shae Padrick for advice on fluorescence anisotropy experiments and Srinivas Somarowthu for assistance in working with ^{32}P-ATP.

References

1. M. I. Hutchings, A. W. Truman, B. Wilkinson, Antibiotics: past, present and future. *Curr Opin Microbiol* **51**, 72-80 (2019).
2. S. Joshi, A. Shallal, M. Zervos, Vancomycin-Resistant Enterococci: Epidemiology, Infection Prevention, and Control. *Infect Dis Clin North Am* **35**, 953-968 (2021).
3. E. Tacconelli, N. Magrini (2017) Global Priority List of Antibiotic-Resistant Bacteria to Guide Research, Discovery, and Development of New Antibiotics. (World Health Organization).
4. T. O'Driscoll, C. W. Crank, Vancomycin-resistant enterococcal infections: epidemiology, clinical manifestations, and optimal management. *Infect Drug Resist* **8**, 217-230 (2015).
5. L. B. Rice, Federal funding for the study of antimicrobial resistance in nosocomial pathogens: no ESKAPE. *J Infect Dis* **197**, 1079-1081 (2008).
6. T. D. Bugg *et al.*, Molecular basis for vancomycin resistance in Enterococcus faecium BM4147: biosynthesis of a depsipeptide peptidoglycan precursor by vancomycin resistance proteins VanH and VanA. *Biochemistry* **30**, 10408-10415 (1991).
7. C. T. Walsh, S. L. Fisher, I. S. Park, M. Prahalad, Z. Wu, Bacterial resistance to vancomycin: five genes and one missing hydrogen bond tell the story. *Chem Biol* **3**, 21-28 (1996).
8. M. I. Hutchings, H. J. Hong, M. J. Buttner, The vancomycin resistance VanRS two-component signal transduction system of Streptomyces coelicolor. *Mol Microbiol* **59**, 923-935 (2006).
9. R. Dutta, M. Inouye, GHKL, an emergent ATPase/kinase superfamily. *Trends Biochem Sci* **25**, 24-28 (2000).
10. R. Dutta, L. Qin, M. Inouye, Histidine kinases: diversity of domain organization. *Mol Microbiol* **34**, 633-640 (1999).
11. J. Cheung, W. A. Hendrickson, Sensor domains of two-component regulatory systems. *Curr Opin Microbiol* **13**, 116-123 (2010).
12. J. Perry, K. Koteva, G. Wright, Receptor domains of two-component signal transduction systems. *Mol Biosyst* **7**, 1388-1398 (2011).
13. C. S. Hughes, E. Longo, M. K. Phillips-Jones, R. Hussain, Characterisation of the selective binding of antibiotics vancomycin and teicoplanin by the VanS receptor regulating type A vancomycin resistance in the enterococci. *Biochim Biophys Acta Gen Subj* **1861**, 1951-1959 (2017).
14. C. S. Hughes, E. Longo, M. K. Phillips-Jones, R. Hussain, Quality control and biophysical characterisation data of VanSA. *Data in brief* **14**, 41-47 (2017).
15. R. Hussain *et al.*, Purification of bacterial membrane sensor kinases and biophysical methods for determination of their ligand and inhibitor interactions. *Biochem Soc Trans* **44**, 810-823 (2016).
16. K. Koteva *et al.*, A vancomycin photoprobe identifies the histidine kinase VanSsc as a vancomycin receptor. *Nature chemical biology* **6**, 327-329 (2010).
17. M. K. Phillips-Jones *et al.*, Hydrodynamics of the VanA-type VanS histidine kinase: an extended solution conformation and first evidence for interactions with vancomycin. *Sci Rep* **7**, 46180 (2017).
18. M. K. Phillips-Jones *et al.*, Full hydrodynamic reversibility of the weak dimerization of vancomycin and elucidation of its interaction with VanS monomers at clinical concentration. *Sci Rep* **7**, 12697 (2017).

19. N. E. Allen, J. N. Hobbs, Jr., Induction of vancomycin resistance in Enterococcus faecium by non-glycopeptide antibiotics. *FEMS Microbiol Lett* **132**, 107-114 (1995).
20. M. Baptista, F. Depardieu, P. Courvalin, M. Arthur, Specificity of induction of glycopeptide resistance genes in Enterococcus faecalis. *Antimicrob Agents Chemother* **40**, 2291-2295 (1996).
21. S. Handwerger, A. Kolokathis, Induction of vancomycin resistance in Enterococcus faecium by inhibition of transglycosylation. *FEMS Microbiol Lett* **58**, 167-170 (1990).
22. A. T. Ulijasz, A. Grenader, B. Weisblum, A vancomycin-inducible lacZ reporter system in Bacillus subtilis: induction by antibiotics that inhibit cell wall synthesis and by lysozyme. *J Bacteriol* **178**, 6305-6309 (1996).
23. R. M. Garavito, S. Ferguson-Miller, Detergents as tools in membrane biochemistry. *J Biol Chem* **276**, 32403-32406 (2001).
24. Z. Yang *et al.*, Membrane protein stability can be compromised by detergent interactions with the extramembranous soluble domains. *Protein Sci* **23**, 769-789 (2014).
25. A. M. Seddon, P. Curnow, P. J. Booth, Membrane proteins, lipids and detergents: not just a soap opera. *Biochim Biophys Acta* **1666**, 105-117 (2004).
26. I. G. Denisov, Y. V. Grinkova, A. A. Lazarides, S. G. Sligar, Directed self-assembly of monodisperse phospholipid bilayer Nanodiscs with controlled size. *J Am Chem Soc* **126**, 3477-3487 (2004).
27. T. K. Ritchie *et al.*, Chapter 11 - Reconstitution of membrane proteins in phospholipid bilayer nanodiscs. *Methods Enzymol* **464**, 211-231 (2009).
28. R. Gao, A. M. Stock, Biological insights from structures of two-component proteins. *Annu Rev Microbiol* **63**, 133-154 (2009).
29. G. D. Wright, T. R. Holman, C. T. Walsh, Purification and characterization of VanR and the cytosolic domain of VanS: a two-component regulatory system required for vancomycin resistance in Enterococcus faecium BM4147. *Biochemistry* **32**, 5057-5063 (1993).
30. F. Depardieu, P. Courvalin, T. Msadek, A six amino acid deletion, partially overlapping the VanSB G2 ATP-binding motif, leads to constitutive glycopeptide resistance in VanB-type Enterococcus faecium. *Mol Microbiol* **50**, 1069-1083 (2003).
31. E. C. Upton, L. J. Maciunas, P. J. Loll, Vancomycin does not affect the enzymatic activities of purified VanSA. *PloS one* **14**, e0210627 (2019).
32. H. K. Carlson *et al.*, Use of a semisynthetic epitope to probe histidine kinase activity and regulation. *Anal Biochem* **397**, 139-143 (2010).
33. C. M. Barbieri, A. M. Stock, Universally applicable methods for monitoring response regulator aspartate phosphorylation both in vitro and in vivo using Phos-tag-based reagents. *Anal Biochem* **376**, 73-82 (2008).
34. E. Kinoshita, E. Kinoshita-Kikuta, T. Koike, The Cutting Edge of Affinity Electrophoresis Technology. *Proteomes* **3**, 42-55 (2015).
35. C. P. Zschiedrich, V. Keidel, H. Szurmant, Molecular Mechanisms of Two-Component Signal Transduction. *J Mol Biol* **428**, 3752-3775 (2016).
36. J. T. Henry, S. Crosson, Ligand-binding PAS domains in a genomic, cellular, and structural context. *Annu Rev Microbiol* **65**, 261-286 (2011).
37. E. C. Stuffle, M. S. Johnson, K. J. Watts, PAS domains in bacterial signal transduction. *Curr Opin Microbiol* **61**, 8-15 (2021).
38. P. Rotsides *et al.*, Novel diazirine photoprobes for the identification of vancomycin-binding proteins. biorXiv [Preprint] (2023). https://www.biorxiv.org/content/10.1101/2023.06.15.545140v1 (accessed 20 June 2023).

39. E. Ishii, Y. Eguchi, Diversity in Sensing and Signaling of Bacterial Sensor Histidine Kinases. *Biomolecules* **11** (2021).
40. C. Chang *et al.*, Extracytoplasmic PAS-like domains are common in signal transduction proteins. *J Bacteriol* **192**, 1156-1159 (2010).
41. T. Boldog, S. Grimme, M. Li, S. G. Sligar, G. L. Hazelbauer, Nanodiscs separate chemoreceptor oligomeric states and reveal their signaling properties. *Proc Natl Acad Sci U S A* **103**, 11509-11514 (2006).
42. B. Wang, A. Zhao, R. P. Novick, T. W. Muir, Activation and inhibition of the receptor histidine kinase AgrC occurs through opposite helical transduction motions. *Molecular cell* **53**, 929-940 (2014).
43. P. Hornschemeyer, V. Liss, R. Heermann, K. Jung, S. Hunke, Interaction Analysis of a Two-Component System Using Nanodiscs. *PloS one* **11**, e0149187 (2016).
44. D. Samanta, J. Widom, P. P. Borbat, J. H. Freed, B. R. Crane, Bacterial Energy Sensor Aer Modulates the Activity of the Chemotaxis Kinase CheA Based on the Redox State of the Flavin Cofactor. *J Biol Chem* **291**, 25809-25814 (2016).
45. T. Affandi, M. M. McEvoy, Mechanism of metal ion-induced activation of a two-component sensor kinase. *Biochem J* **476**, 115-135 (2019).
46. M. Ghosh *et al.*, Lipid-Mediated Regulation of Embedded Receptor Kinases via Parallel Allosteric Relays. *Biophys J* **112**, 643-654 (2017).
47. Z. A. Maschmann, T. K. Chua, S. Chandrasekaran, H. Ibanez, B. R. Crane, Redox properties and PAS domain structure of the Escherichia coli energy sensor Aer indicate a multistate sensing mechanism. *J Biol Chem* **298**, 102598 (2022).
48. Q. Xie *et al.*, Discovery of quorum quenchers targeting the membrane-embedded sensor domain of the Staphylococcus aureus receptor histidine kinase, AgrC. *Chem Commun (Camb)* **56**, 11223-11226 (2020).
49. S. Jordan, M. I. Hutchings, T. Mascher, Cell envelope stress response in Gram-positive bacteria. *FEMS Microbiol Rev* **32**, 107-146 (2008).
50. T. Mascher, Bacterial (intramembrane-sensing) histidine kinases: signal transfer rather than stimulus perception. *Trends Microbiol* **22**, 559-565 (2014).
51. E. C. Hobbs, X. Yin, B. J. Paul, J. L. Astarita, G. Storz, Conserved small protein associates with the multidrug efflux pump AcrB and differentially affects antibiotic resistance. *Proc Natl Acad Sci U S A* **109**, 16696-16701 (2012).
52. A. M. Lippa, M. Goulian, Feedback inhibition in the PhoQ/PhoP signaling system by a membrane peptide. *PLoS Genet* **5**, e1000788 (2009).
53. G. Storz, Y. I. Wolf, K. S. Ramamurthi, Small proteins can no longer be ignored. *Annu Rev Biochem* **83**, 753-777 (2014).
54. V. W. Rowlett *et al.*, Impact of Membrane Phospholipid Alterations in Escherichia coli on Cellular Function and Bacterial Stress Adaptation. *J Bacteriol* **199** (2017).
55. R. Rashid *et al.*, Comprehensive analysis of phospholipids and glycolipids in the opportunistic pathogen Enterococcus faecalis. *PloS one* **12**, e0175886 (2017).
56. H. Piepenbreier, A. Diehl, G. Fritz, Minimal exposure of lipid II cycle intermediates triggers cell wall antibiotic resistance. *Nat Commun* **10**, 2733 (2019).
57. A. A. Guffey, P. J. Loll, Regulation of Resistance in Vancomycin-Resistant Enterococci: The VanRS Two-Component System. *Microorganisms* **9** (2021).
58. S. D. Weeks, M. Drinker, P. J. Loll, Ligation independent cloning vectors for expression of SUMO fusions. *Protein Expr Purif* **53**, 40-50 (2007).
59. L. Dobson, I. Remenyi, G. E. Tusnady, CCTOP: a Consensus Constrained TOPology prediction web server. *Nucleic Acids Res* **43**, W408-412 (2015).

60. E. S. Poole, C. M. Brown, W. P. Tate, The identity of the base following the stop codon determines the efficiency of in vivo translational termination in Escherichia coli. *EMBO J* **14**, 151-158 (1995).
61. Anonymous, Determination of Total Phosphorus. https://avantilipids.com/tech-support/analytical-procedures/determination-of-total-phosphorus [Preprint] https://avantilipids.com/tech-support/analytical-procedures/determination-of-total-phosphorus
62. C. H. Fiske, Y. Subbarow, The Colorimetric Determination of Phosphorous. *J Biol Chem* **66**, 374-389 (1925).
63. H. Bao, F. Duong, C. S. Chan, A step-by-step method for the reconstitution of an ABC transporter into nanodisc lipid particles. *Journal of visualized experiments : JoVE* 10.3791/3910, e3910 (2012).
64. J. Jumper *et al.*, Highly accurate protein structure prediction with AlphaFold. *Nature* **596**, 583-589 (2021).

Figures

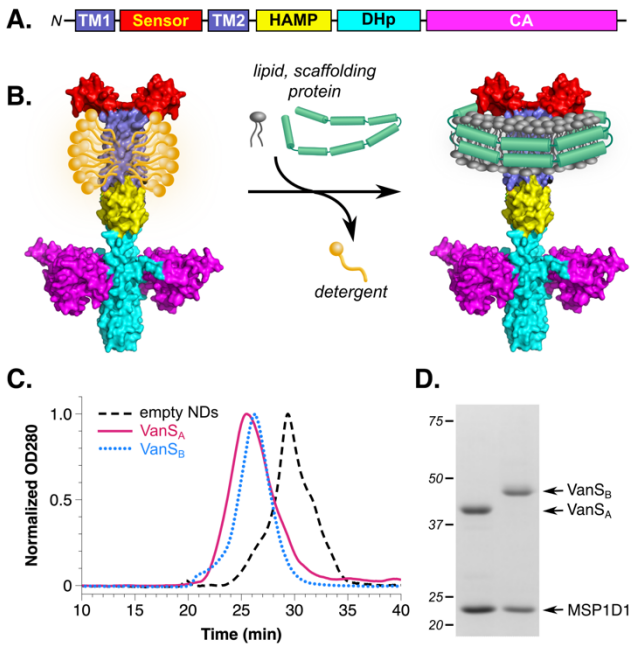

Figure 1. Reconstitution of VanS proteins into nanodiscs. (*A*) Schematic representation of a typical VanS protein. Two transmembrane helices (TM1 & TM2) flank a periplasmic sensor domain, the length of which varies significantly among different VanS proteins. The cytoplasmic portion of the protein contains a membrane-proximal region, which typically forms a HAMP domain, followed by the DHp and CA domains. (*B*) For nanodisc formation, detergent-solubilized protein is incubated with lipids and scaffolding protein, after which detergent is removed, triggering the spontaneous formation of protein-belted lipid discs around the hydrophobic face of the protein. The protein model shown represents the structure of full-length VanS$_A$, as predicted by AlphaFold (64). (*C*) Size-exclusion chromatograms reveal that nanodiscs containing either VanS$_A$ or VanS$_B$ elute earlier than empty nanodiscs formed under identical conditions, indicating size increases consistent with the incorporation of VanS proteins. (*D*) Coomassie-stained denaturing SDS-PAGE gels showing purified VanS$_A$ and VanS$_B$ nanodisc preparations, and indicating that these preparations contain approximately equimolar amounts of VanS and the scaffolding protein MSP1D1.

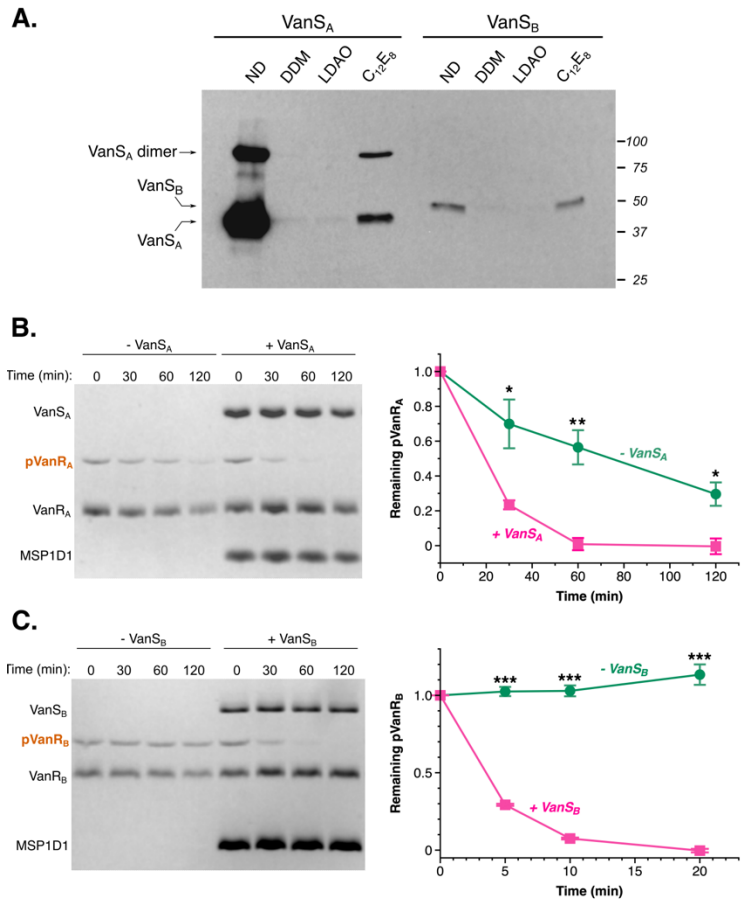

Figure 2. Enzymatic activities of $VanS_A$ and $VanS_B$ proteins. (*A*) VanS activity is strongly sensitive to the membrane mimetic environment. In each reaction, 0.3 μM VanS was incubated with 1 mM ATPγS for 30 minutes. The thio-phospho-histidine was then alkylated with *p*-nitrobenzyl mesylate (PNBM), which was subsequently detected by Western blot. Equal amounts of VanS protein are loaded in each lane. Both VanS proteins show very little activity in the presence of the detergents DDM and LDAO, and modest activity in C12E8. $VanS_A$ activity increases drastically when the protein is reconstituted in nanodiscs (ND), whereas the corresponding increase in $VanS_B$ activity is markedly lower. (*B*) Dephosphorylation activity of $VanS_A$. Phosphorylated $VanR_A$ was incubated ± $VanS_A$-containing nanodiscs, and the time-dependent decrease in phosphorylation was monitored using Phos-Tag™ gels. A representative gel is shown at left, with the quantitation shown at right. Asterisks represent *p*-values calculated using an unpaired T-test; *, *p*-value < 0.05; **, *p*-value < 0.01; ***, *p*-value < 0.0001 ($n = 3$). (*C*) Dephosphorylation activity of $VanS_B$, monitored as described for panel (B). Phospho-$VanR_B$ shows greater intrinsic stability than phospho-$VanR_A$, consistent with the observation that it is possible to isolate $VanR_B$ in a partially phosphorylated form after expression in *E. coli* (SI Appendix, Fig. S8).

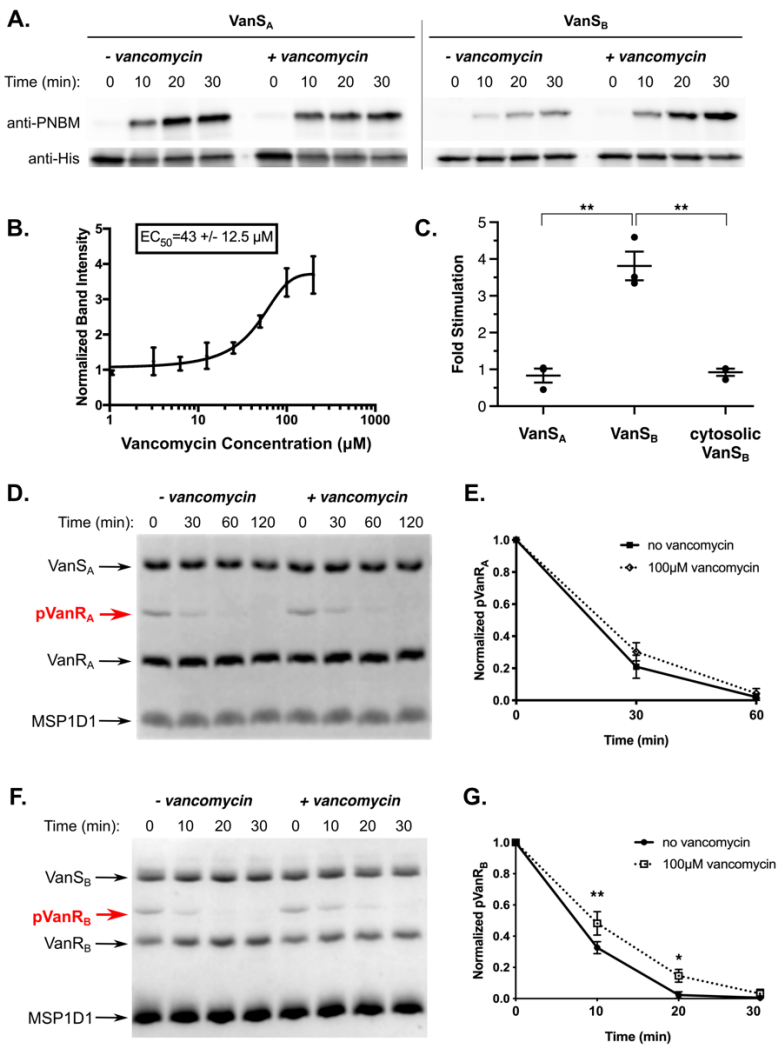

Figure 3. Effect of vancomycin on VanS activities. (*A*) Time course of autophosphorylation activity for $VanS_A$ and $VanS_B$, ± 100 μM vancomycin. (*B*) Dose dependence for vancomycin stimulation of $VanS_B$ autophosphorylation activity. (*C*) Quantitation of vancomycin's stimulation of autophosphorylation activity for $VanS_A$ and $VanS_B$ (reconstituted in nanodiscs), as well as for the cytosolic domain of $VanS_B$. (*D*) A representative Phos-tag™ gel demonstrating that 100 μM vancomycin has no effect on the dephosphorylation activity of $VanS_A$. (*E*) Quantitation of three dephosphorylation experiments for $VanS_A$. Addition of vancomycin produces no statistically significant difference in activity. (*F*) A representative Phos-tag™ gel demonstrating that 100 μM vancomycin has a modest inhibitory effect on the dephosphorylation activity of $VanS_B$. (*G*) Quantitation of three dephosphorylation experiments for $VanS_B$. *, *p*-value < 0.05; **, *p*-value < 0.01.

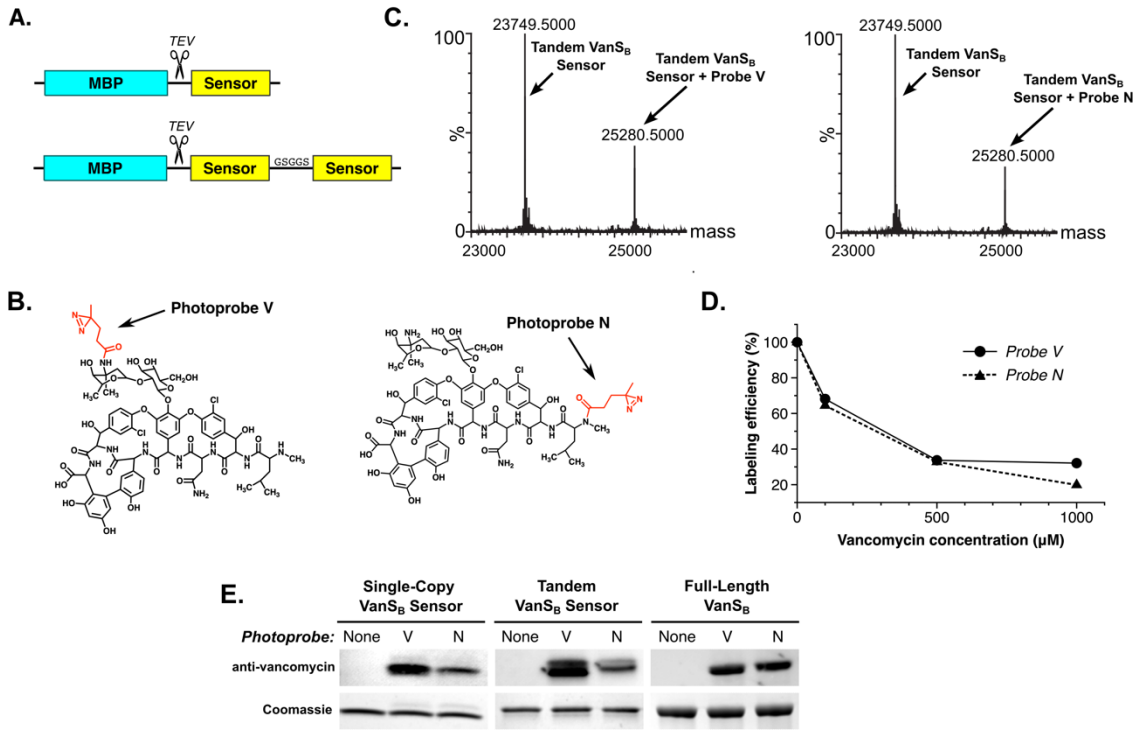

Figure 4. The $VanS_B$ periplasmic sensor domain can be labeled with vancomycin-based photoprobes. (*A*) The $VanS_B$ periplasmic sensor domain (residues 31-132) was expressed as a cleavable fusion with MBP, in both single-copy and tandem forms, and purified to homogeneity (SI Appendix, Fig. S4). (B) Two photoprobes were used, in which a photo-active diazirine was attached to either the antibiotic's vancosamine sugar (Photoprobe V) or its N-terminus (Photoprobe N). (C) Mass spectrometric evidence that both photoprobes label the purified tandem sensor-domain construct. (D) Vancomycin competes with both photoprobes for binding to the tandem sensor domain. (E) Confirmation of photolabeling using an anti-vancomycin Western-blot assay, showing labeling of both the isolated single-copy and tandem sensor domains, as well as full-length $VanS_B$. Coomassie-stained gels serve as loading controls. Photoprobe N typically labels $VanS_B$ constructs less efficiently than Photoprobe V, as judged by both Western blotting and mass spectrometry (see panel (C)); this may reflect differences in the diazirine group's proximity to the protein, as determined by the conformation of the bound antibiotic.

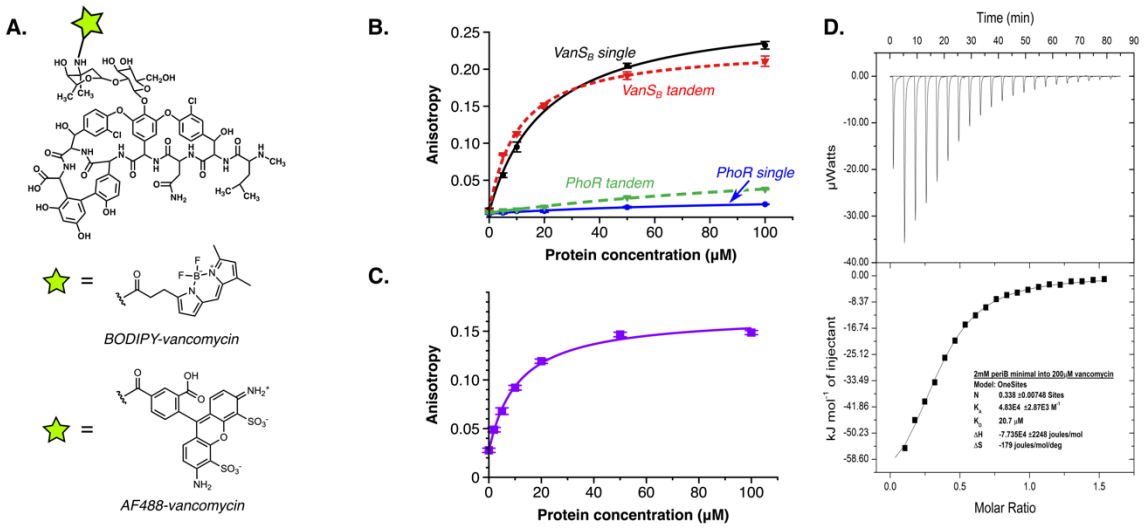

Figure 5. Vancomycin binds directly to the periplasmic sensor domain of VanS$_B$. (A) Two different fluorescently labeled vancomycin derivatives used for fluorescence anisotropy measurements. (B) BODIPY-vancomycin binds to both the single and tandem sensor-domain constructs of VanS$_B$. In contrast, single and tandem constructs of the PhoR negative control fail to bind the antibiotic. (C) The VanS$_B$ tandem sensor-domain construct also binds AF488-vancomycin, confirming that the binding observed with BODIPY-vancomycin is not fluorophore-specific. (D) Isothermal titration calorimetry confirms vancomycin binding by the single-copy VanS$_B$ sensor-domain construct. The related glycopeptide antibiotic teicoplanin fails to bind to the sensor domain (SI Appendix, Fig. S5), which is consistent with the known behavior of type-B VRE.